MEDICAL SCIENCE MONITOR

LAB/IN VITRO RESEARCH

e-ISSN 1643-3750
© Med Sci Monit, 2017; 23: 4723-4732
DOI: 10.12659/MSM.902538

Received: 2016.11.25
Accepted: 2017.04.10
Published: 2017.10.02

Nano-Hydroxyapatite-Derived Drug and Gene Co-Delivery System for Anti-Angiogenesis Therapy of Breast Cancer

Authors' Contribution:
Study Design A
Data Collection B
Statistical Analysis C
Data Interpretation D
Manuscript Preparation E
Literature Search F
Funds Collection G

ABCDEFG 1 Lina Zhao
BCD 2 Wenhui Zhao
ADF 3 Ye Liu
ADF 1 Xue Chen
CD 1 Yan Wang

1 Department of Hematology, Tumor Hospital Affiliated to Harbin Medical University, Harbin, Heilongjiang, P.R. China
2 Department of Internal Medicine, Tumor Hospital Affiliated to Harbin Medical University, Harbin, Heilongjiang, P.R. China
3 Department of Immunology, Harbin Medical University, Harbin, Heilongjiang, P.R. China

Corresponding Author: Lina Zhao, e-mail: linazhao0716@163.com
Source of support: Departmental sources

Background: Breast cancer is among the deadliest cancers across the world and is responsible for countless deaths. There is an urgent need for co-delivery systems which can simultaneously transport both drug and gene into a single cancer cell with low toxicity and high anti-angiogenesis efficiency.

Material/Methods: In the present study, well-formed amine-functionalized hydroxyapatite nanoparticles based on combined angiogenesis therapy for breast cancer were successfully constructed for the simultaneous delivery of p53 and candesartan (CD) (p53/CD/NHAP).

Results: *In vitro* and *in vivo* experiments revealed that p53/CD/NHAP can effectively transfer the p53 gene and deliver the loaded CD to achieve preferable anti-breast cancer effect both at the cellular level and in tumor-bearing mice. This may possibly be due to the combined anti-angiogenic mechanisms of p53 and CD via different pathways.

Conclusions: p53/CD/NHAP might be a candidate carrier for efficient anti-angiogenesis therapy of breast cancer.

MeSH Keywords: **Angiogenesis Inhibitors • Angiotensin II Type 1 Receptor Blockers • Genes, p53 • Hydroxyapatites • Inflammatory Breast Neoplasms**

Full-text PDF: https://www.medscimonit.com/abstract/index/idArt/902538

3530 — 6 39

Indexed in: [Current Contents/Clinical Medicine] [SCI Expanded] [ISI Alerting System] [ISI Journals Master List] [Index Medicus/MEDLINE] [EMBASE/Excerpta Medica] [Chemical Abstracts/CAS] [Index Copernicus]

Background

Breast cancer is among the deadliest cancers across the world and is responsible for countless deaths. According to the World Cancer Report, breast cancer caused 458 503 deaths worldwide in the year 2008 alone, and more in the following years.

It has been well documented that the growth of solid neoplasms is always accompanied by neovascularization. Many previous works have proved the positive association between the growth of solid malignant tumors and new vessels [1–3]. In recent years, it has been widely appreciated that the population of tumor cells and the population of capillary endothelial cells within a neoplasm may constitute a highly integrated ecosystem which plays an important role in tumor progression and accounts for the lethality of cancers [4–6].

Given the role of angiogenesis in tumor growth and progression, targeting tumor vasculature as a therapeutic means has been long proposed and deemed as a practical approach to cure cancer [7]. As a result, anti-angiogenesis therapy applied in breast cancer has been widely adopted, since breast cancer has been identified to be a malignancy that tends to spread quickly at the late stage due to angiogenesis effects [9–10]. This protocol targets the key angiogenic factors, including vascular endothelial growth factor (VEGF) [11] and matrix metalloproteinases (MMPs) [12], to block the angiogenesis-related cellular pathways. Among angiogenic activators, VEGF was proven to be one of the key regulators of both physiological and pathological angiogenesis [13]. As a result, anti-angiogenesis breast cancer therapy based on VEGF targeting has become the focus of related research [14–16].

To date, multiple positive results have shown that angiotensin II (Ang II) can play an important role not only in blood pressure regulation, but also in modulation of tumor angiogenesis and progression, possibly by regulating VEGF via angiotensin II type 1 receptor (AT_1R) [17]. Moreover, AT_1R overexpression in various neoplastic cells (e.g., breast and ovarian carcinoma cells) [18], has been well established for years. As a result, AT_1R could be considered as a noteworthy target in anticancer therapy. Restoring p53 function within cancer cells using drug delivery systems (DDS) has been found to increase the sensitivity of cancer cells to anticancer drugs [19–22]. More interestingly, further studies revealed that tumor-associated angiogenesis can be positively inhibited by the VEGF down-regulation effects of p53 gene by either direct interaction or indirect pathways [23–25].

Although combination anti-angiogenic therapy of 2 traditional chemotherapeutics via different action mechanisms showed advantages to some extent [26], its application was sometimes severely hindered by adverse effects and/or multidrug resistance (MDR). The combination of drug and gene therapy may offer a second paradigm in anti-angiogenic breast cancer treatment [27]. Therefore, co-delivery systems which can simultaneously transport an anticancer drug and a gene into a single cancer cell, with low toxicity and high therapy efficiency, should be developed.

Nanomaterials capable of fulfilling the co-delivery mission include organic ones such as polyplexes [28] and cationic micelles [29], and inorganic ones such as silica [30] and hydroxyapatite nanoparticles (HAP) [31]. HAP is deemed as a feasible candidate and possess many characteristics desired of an ideal drug and gene co-delivery vector, such as low cytotoxicity, large surface area, and ease of fabrication and modification [32]. Here, we report that we have successfully developed a DDS based on amine-functionalized hydroxyapatite (NHAP) nanoparticles. Candesartan (CD) is an angiotensin II type 1 receptor blocker (ARB) with stronger affinity for AT_1R of tumor cells than other ARBs [33]. CD, together with p53 plasmid, were chosen as the therapeutic drug and gene, respectively. Subsequently, CD and p53 were loaded onto NHAP to construct the drug and gene co-delivery system (p53/CD/NHAP). The self-assemblies of p53/CD/NHAP nanoparticles were investigated by their change in particle size, zeta potential, and drug loading efficiency. Gel retardation assay was performed *in vitro* to seek the optimize weight/weight (w/w) ratio of NHAP nanoparticles to p53 plasmid in the formulation of p53/CD/NHAP nanoparticles. Moreover, *in vitro* transfection and anticancer efficiency, together with *in vivo* anticancer assay of p53/CD/NHAP nanoparticles, were also evaluated to further elucidate the positive potential of p53/CD/NHAP nanoparticles in anti-angiogenic breast cancer therapy.

Material and Methods

Preparation of p53/CD/NHAP nanoparticles

Equivalent mole ratio of 3-aminopropyl-triethoxysilane (APS, Sigma-Aldrich, St. Louis, USA) and HAP nanoparticles (Beijing DK Nanotechnology Co., Ltd., Beijing, China) were added into a flask containing the proper amount of mixed solution (ethanol: water=9: 1) and agitated for intensive mixing. After that, solution pH was adjusted to 10 with ammonium hydroxide and the reaction further proceeded for another 3 h. Finally, the NHAP nanoparticles were obtained by centrifugation (5000×g, 10 min, Allegra X-22, Beckman, USA). The precipitation was washed several times with ethanol and desiccated at 50°C under high vacuum until further use.

The prepared NHAP nanoparticles were dispersed in ethanol to obtain a concentration of 10 mg/ml. After that, CD (5 mg) dissolved in chloroform was added into the solution with

Indexed in: [Current Contents/Clinical Medicine] [SCI Expanded] [ISI Alerting System] [ISI Journals Master List] [Index Medicus/MEDLINE] [EMBASE/Excerpta Medica] [Chemical Abstracts/CAS] [Index Copernicus]

agitation. The mixture was agitated for 6 h, followed by another centrifugation to isolate the CD/NHAP nanoparticles from the solution. The precipitation was repeatedly washed with ethanol and chloroform, desiccated, and finally resuspended in distilled water (Merck Millipore, USA).

P53 plasmid obtained from Addgene (Cambridge, USA) was dissolved in HEPES buffer (20 mM, pH 7.4) to get a clear solution (0.1 mg/ml). The plasmid solution was then added dropwise into the aqueous solution of CD/NHAP nanoparticles at the different w/w ratio (NHAP to ANG, 10 to 60) with vortex to form p53/CD/NHAP. The final mixture was allowed to stand for 30 min before use. The particle size and zeta potential of HAP, CD/NHAP, and p53/CD/NHAP nanoparticles were determined by use of the Size and Zeta Potential Analyzer (90Plus, Brookhaven, USA).

The protection potential of NHAP nanoparticles on p53 was evaluated by agarose gel electrophoresis. The p53/CD/NHAP nanoparticles at different w/w ratios (containing 0.2 μg p53 plasmid) were processed as previous reported [34].

The anti-DNase degradation ability of p53 with the protection of NHAP nanoparticles in serum was also determined as reported previously [35].

Drug loading content

The prepared p53/CD/NHAP nanoparticles were collected by centrifugation and dispersed in acetone/methanol (1/1, v/v) with gentle agitation for 24 h. After that, supernate obtained by centrifugation was subjected to HPLC analysis under the same condition as reported previously [27].

In vitro cytotoxicity assay

For cell viability assay of p53/CD/NHAP nanoparticles, MCF-7 (Cell Bank of SIBCB, CAS, Shanghai, China) cells were seeded at the density of 1.0×10^4 cells/well (96-well plates, Corning, USA) and incubated overnight. The primary growth medium was afterwards replaced with 200 μl of serum-free medium, to which different nanoparticles were added to achieve designated concentrations (10, 20, 50, 100, 150, and 200 μg/ml). After different intervals of incubation (24, 48, and 72 h), the cytotoxicity assay was performed according a previous report [36].

In vitro gene transfection studies

The transfection capability of NHAP nanoparticles-mediated reporter gene pEGFP (Addgene, Cambridge, USA) in MCF-7 cells was qualitatively and quantitatively investigated, respectively, in compare to Polyethyleneimine (PEI) 25 KDa (Sigma-Aldrich, St. Louis, MO, USA). Cells seeded at 6-well plates were allowed to grow overnight to reach 80% confluence. The pPEGFP/NHAP nanoparticles and pEGFP/PEI 25K (1: 1, w/w) were diluted with serum-free medium and added to the wells (plasmid concentration: 1 μg/well) at 37°C for 4 h. The primary medium was then discarded and cells were treated with fresh FBS containing medium to culture for another 48 h [34]. Afterwards, the transfected cells were washed thoroughly with PBS, either subjected to observation and photography by fluorescent microscope (OlympusIX51, Japan) or quantified by GFP-positive cells and GFP fluorescence intensity by flow cytometry (Becton Dickinson, USA).

qRT-PCR, Western blotting and ELISA assays

The variation of VEGF mRNA level in the transfected MCF-7 cells using p53/CD/NHAP nanoparticles were determined by qRT-PCR assay, following the protocols reported previously [27]. Expression of VEGF and AT_1R genes at protein level was evaluated by Western blotting as previously reported [37]. VEGF level was further studied by ELISA assay as reported previously [4].

In vivo anticancer study

To further evaluate the performance of p53/CD/NHAP within the living animals, the *in vivo* anticancer study was performed. Female BALB/c nude mice (mean body weight: 16–18 g) were donated from Shanghai Laboratory Animal Center (SLAC, China) and housed in an SPF laboratory room at 22±2°C with access to food and water ad libitum. Six mice were randomly assigned each of the following groups: Group A: saline (control group); B: pEGFP/CD/NHAP nanoparticles; C: p53/NHAP nanoparticles; group D: p53/NHAP nanoparticles plus free CD; and group E: p53/CD/NHAP nanoparticles. The MCF-7 tumor-bearing mouse model was established as reported previously. Briefly, MCF-7 cells were trypsinized and resuspended in PBS. We inoculated 5×10^6 cells/0.1 mL into the mammary fat pad of mice using a 27-gauge syringe. The tumor volume (TV) was calculated as $TV=(width^2\times length)\times0.5$ [38]. When the tumor volume reached approximately 100 mm^3, the mice were injected intravenously via the tail vein at a dose of 50 μg p53 gene and/or 30 μg CD/mouse every 2 days for a 14-day therapeutic period. The dimension of the tumor measured by a caliper and the total body weight was also measured simultaneously. All procedures were in strict accordance with NIH guidance. After the final day of measurement, mice from each group were randomly selected and sacrificed, their tumor tissues were extracted and subjected to H&E staining to compare the anticancer effect of each formulation. Additionally, 3 mice in each group were randomly sacrificed and their tumor tissues were subjected to antibody staining followed by microvessel density (MVD) calculation (number/mm^2) by measuring the number of CD31-positive objects in each specified field as reported previously [27].

Indexed in: [Current Contents/Clinical Medicine] [SCI Expanded] [ISI Alerting System] [ISI Journals Master List] [Index Medicus/MEDLINE] [EMBASE/Excerpta Medica] [Chemical Abstracts/CAS] [Index Copernicus]

A

	Mean particle size (nm)	Zeta potential (mV)
HAP nanoparticles	50.3±6.2	−21.5±2.7
NHAP nanoparticles	60.6±5.6	+30.8±3.9
CD/NHAP nanoparticles	61.2±4.8	+25.2±4.1

B

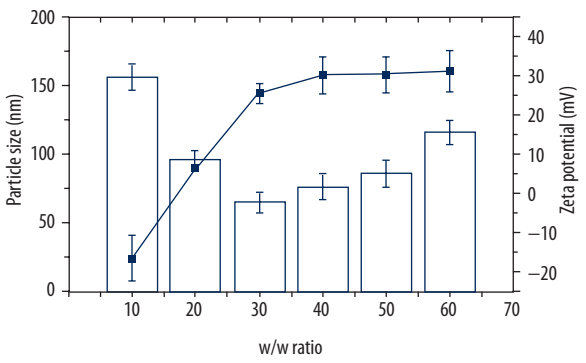

Figure 1. (**A**) Particle size and zeta potential of different nanoparticles. (**B**) Particle size and zeta potential of p53/CD/NHAP nanoparticles at different w/w ratios (NHAP to p53, 10–60). Data are shown as mean ±S.D. (*n*=3).

Results and Discussion

Particle size, zeta potential and drug loading

Particle size and zeta potential play an important role in the performance of the nanoparticles. It has been suggested that particle size smaller than 200 nm is more favorable for anticancer utilization since particles within this range are tend to accumulate at the tumor tissue due to the so-called enhanced permeability and retention (EPR) effect. To deliver gene molecules, the nanoparticles should be positively charged to condense the negatively charged nucleic acid. However, it has been shown that positively charged nanoparticles are more likely to be taken up by cancer cells and the reticuloendothelial system (RES). Strongly positive nanoparticles, such as PEI-derived polyplexes, are usually toxic due to the damage to the cell membrane. Moderate-positive nanoparticles, like chitosan-based ones, in contrast, performed well both *in vitro* and *in vivo*. These results suggested that moderate-positive surface charge may alleviate the cytotoxicity of the nanoparticles and achieve good performance. The comparative particle size and zeta potential of HAP and NHAP nanoparticles were first tested. The particle size measurement revealed that HAP have a diameter of around 50.3 nm and a zeta potential of –21.5 mV (Figure 1A). The negative surface charge may be due to the presence of phosphate group on the surface of HAP nanoparticles. However, after amine functionalization, the surface charge of NHAP nanoparticles reversed to be a positive one of + 30.8 mV. The particle size of NHAP nanoparticles was also increased a little to be 60 nm, indicating the anchoring of additional amine groups on the surface of the HAP nanoparticles. After drug loading of CD, the obtained CD/NHAP nanoparticles are still positively charged with slightly decreased value, suggesting that the CD molecules with negative carboxyl groups are entrapped both within the core and onto the surface of the NHAP nanoparticles. The final obtained p53/CD/NHAP nanoparticles, their particle size, and zeta potential vary with the change of w/w ratio between p53 and CD/NHAP nanoparticles. It was reported that the w/w ratio exerts a significant effect on transfection efficiency of the finally constructed delivery system [39]. As depicted in Figure 1B, when w/w ratio reached 10, the particle size of p53/CD/NHAP nanoparticles was significantly increased to 156.4 nm with a reversed surface charge of – 16.54 mV. The excess presence of p53 (negatively charged) at the surface of amine-functionalized CD/NHAP nanoparticles might be responsible for reversing the zeta potential and increasing the particle size. As expected, the particle size decreased synchronously with the increase of w/w ratio within the first stage, and reached a minimum value (~65 nm) at the w/w ratio of 30, which might be due to the formation of condensed and stable complexes p53/CD/NHAP nanoparticles, and a further increase in w/w ratio showed a positive correlation with particle size. Moreover, the zeta potential of p53/CD/NHAP nanoparticles increased with increasing w/w ratios, and finally stabilized at around + 30.38 mV at the ratio of 30.

Gel retardation assay, serum stability, and drug loading of p53/CD/NHAP nanoparticles

The prerequisite requirements for successful gene delivery of cationic vectors are plasmid binding and protecting capabilities. The plasmid-condensing ability of NHAP nanoparticles was verified by gel retardation assay. As shown in Figure 2A, free p53 showed no retardation. However, at the ratio of 10, NHAP nanoparticles showed certain p53 biding ability with a relatively weaker band compared to free p53. Moreover, with the increase of w/w ratio, NHAP nanoparticles demonstrated increasing p53 binding ability, which achieve complete and satisfying retardation of p53 at the ratio of over 30. The protective effect of the NHAP nanoparticles on p53 against serum nucleases degradation was assessed by the co-culture of NHAP nanoparticles with serum (Figure 2B). Naked p53 was completely degraded after being incubated in FBS for 24 h. However, NHAP nanoparticles showed good protective effect

Indexed in: [Current Contents/Clinical Medicine] [SCI Expanded] [ISI Alerting System] [ISI Journals Master List] [Index Medicus/MEDLINE] [EMBASE/Excerpta Medica] [Chemical Abstracts/CAS] [Index Copernicus]

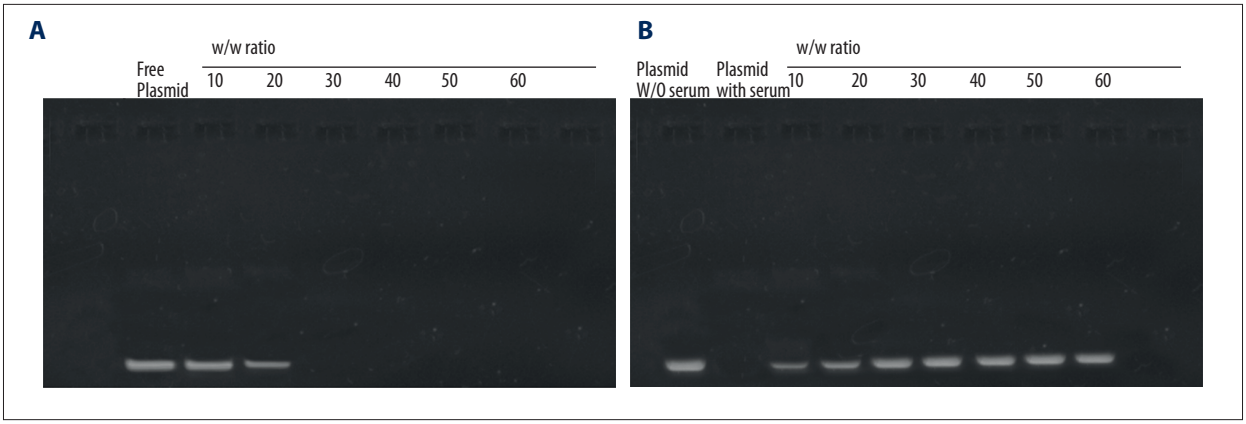

Figure 2. (**A**) p53 binding assay of p53/CD/NHAP nanoparticles at various w/w ratios. (**B**) p53 protecting assay of p53/CD/NHAP nanoparticles at various w/w ratios.

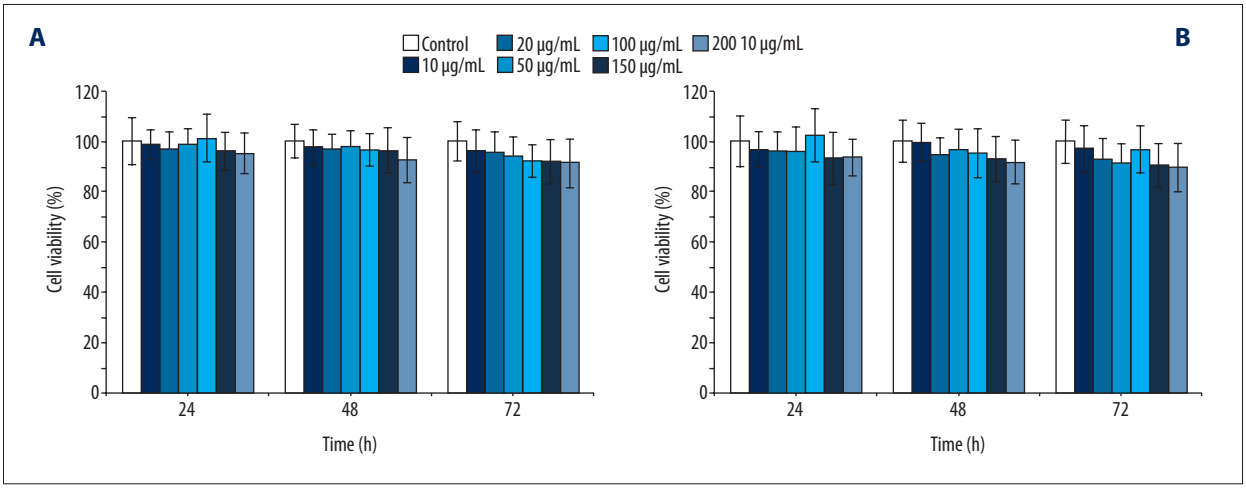

Figure 3. Cell viabilities of MCF-7 (**A**) and MCF10A (**B**) cells incubated with drug-free NHAP nanoparticles at various concentrations for 24, 48 and 72 h, respectively. Data are expressed as mean ±S.D. (*n*=5).

on p53 at all tested ratios, and higher ratios tended to have stronger protective capability. NHAP nanoparticles reached full protection of p53 at the ratio of 30, which was supported by comparable and evident bands to control, which was consistent with the results obtained from the binding assay.

In summary, it was inferred that p53/CD/NHAP nanoparticles at the w/w ratio of 30 exerted desirable surface charge, proper particle size, effective p53 condensation and protection capability, and were selected as the optimal nanoparticles in the following studies. The drug-loading efficiency of NHAP nanoparticles at the ratio of 30 was calculated to be 12.18±4.26% (data not shown).

In vitro cell viability assays

The cytotoxicity of drug-free NHAP nanoparticles was assessed by standard MTT assay. As shown in Figure 3, the cytotoxicity of NHAP nanoparticles was dose-dependent. At the highest NHAP nanoparticles concentration of 200 μg/ml, there was still over 90% of cell viability remaining after 72 h of incubation, suggesting their low cytotoxicity. Compared with cytotoxicity in the groups which were incubated with the NHAP nanoparticles for 24 h, cells incubated for 48 h and 72 h demonstrated comparable cell viability without any significant difference observed. This was beneficial for p53/CD/NHAP nanoparticles to act as a delivery system. Since p53/CD/NHAP nanoparticles at the highest concentration still demonstrated low cytotoxicity, it was inferred that all the cancer therapeutic effects in the following experiments were due to the angiogenesis of either CD or p53 or the combination of them without interference from the carrier.

Transfection capability of pEGFP/CD/NHAP nanoparticles

To evaluate the transfection capability of CD/NHAP nanoparticles, pEGFP plasmid encoding GFP was employed as an alternative to p53 to fulfill this purpose in a simple way, since GFP

Indexed in: [Current Contents/Clinical Medicine] [SCI Expanded] [ISI Alerting System] [ISI Journals Master List] [Index Medicus/MEDLINE] [EMBASE/Excerpta Medica] [Chemical Abstracts/CAS] [Index Copernicus]

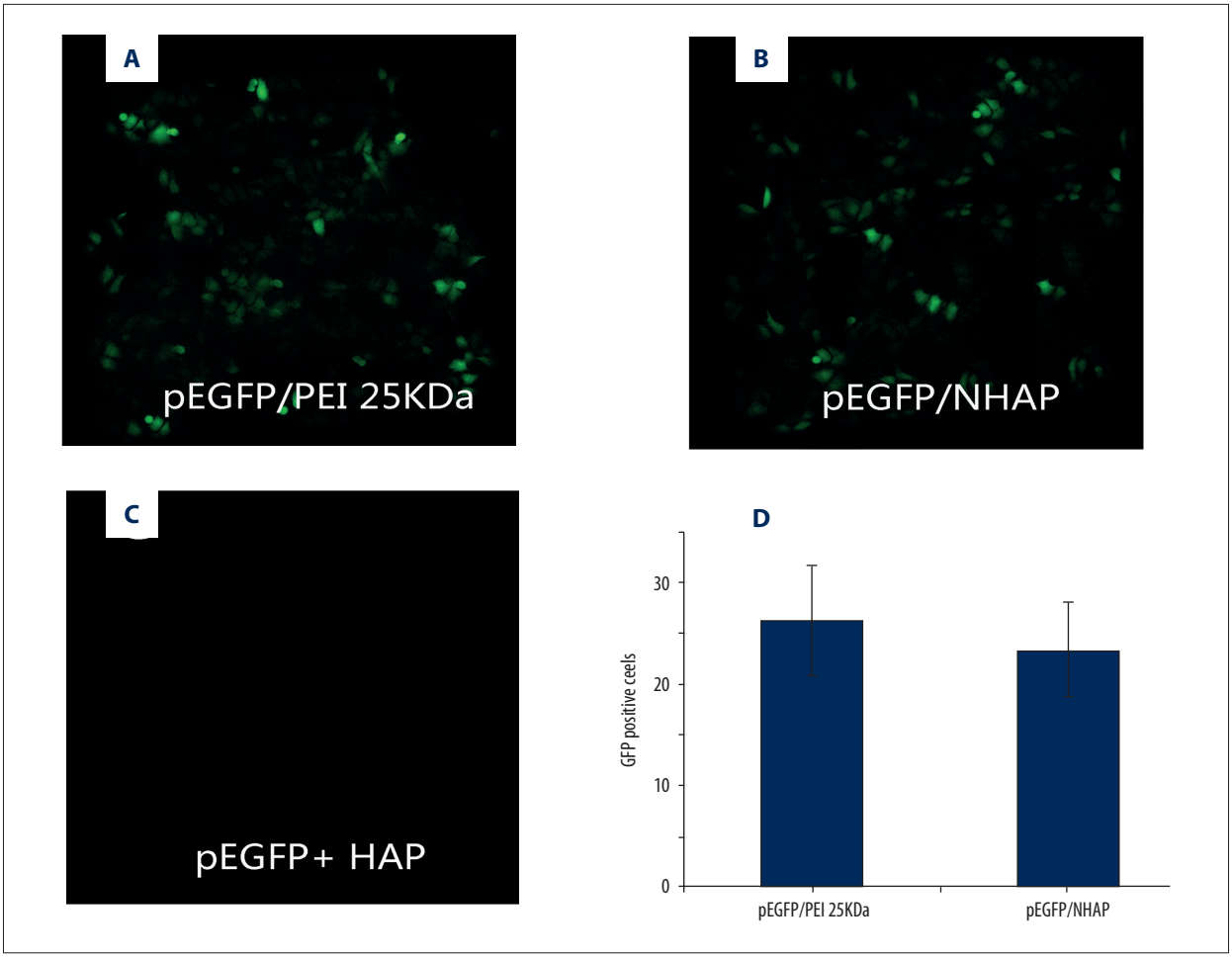

Figure 4. Green fluorescent protein (GFP) expression efficiency in MCF-7 cells using different formulations. Fluorescence images of cells transfected with (**A**) pEGFP/CD/NHAP nanoparticles (w/w=30), with (**B**) pEGFP/PEI 25KDa (w/w=1), and (**C**) naked pEGFP plus HAP. (**D**) Flow cytometric analysis of pEGFP/CD/NHAP nanoparticles and pEGFP/PEI 25KDa. Data are shown as mean ±S.D. (n=5).

can easily be observed and quantified. To determine the comparative transfection capability of pEGFP/CD/NHAP nanoparticles, PEI 25KDa as a generally recognized polymer with exerts high transfection efficiency *in vitro* was employed. pEGFP/PEI 25KDa complexes at the optimal w/w ratio of 1 with low cytotoxicity and high transfection efficiency were employed as control [35]. It can be concluded from Figure 4A–4C that pEGFP/PEI 25KDa complexes demonstrated the highest transfection efficiency, while free p53 without any protection showed no transfection. We also observed that pEGFP/CD/NHAP nanoparticles possessed comparable transfection efficiency to pEGFP/PEI 25KDa complexes with relatively strong GFP signals (green color). To further confirm the results, flow cytometry was applied to quantitative determine the transfection efficiency of pEGFP/PEI 25KDa complexes and pEGFP/CD/NHAP nanoparticles (free pEGFP plasmid was used to normalize the transfection efficiency). As depicted in Figure 4D, pEGFP/PEI 25KDa complexes successfully transfected 26.07% of the total cells, while there were 23.26% positive cells in pEGFP/CD/NHAP nanoparticles. There was no significant difference observed between these 2 formulations, which provided decisive evidence that pEGFP/CD/NHAP nanoparticles can effectively raise the transfection efficiency of pEGFP plasmid. In summary, NHAP nanoparticles exerted comparative transfection capability to the criterion standard PEI 25K; as a result, good p53 transfection and anti-angiogenesis effects can be expected.

In vitro anti-angiogenesis efficiency

VEGF has been widely recognized as one of the most important cytokines in angiogenesis and was proved to be a candidate target for cancer therapy [6]. The expression of VEGF at mRNA and protein level in p53/CD/NHAP nanoparticles transfected MCF-7 cells was evaluated to revel the *in vitro* anti-angiogenesis efficiency of p53/CD/NHAP nanoparticles. We first used 100 nM of Ang II and assessed its effect on mRNA expression

Indexed in: [Current Contents/Clinical Medicine] [SCI Expanded] [ISI Alerting System] [ISI Journals Master List] [Index Medicus/MEDLINE] [EMBASE/Excerpta Medica] [Chemical Abstracts/CAS] [Index Copernicus]

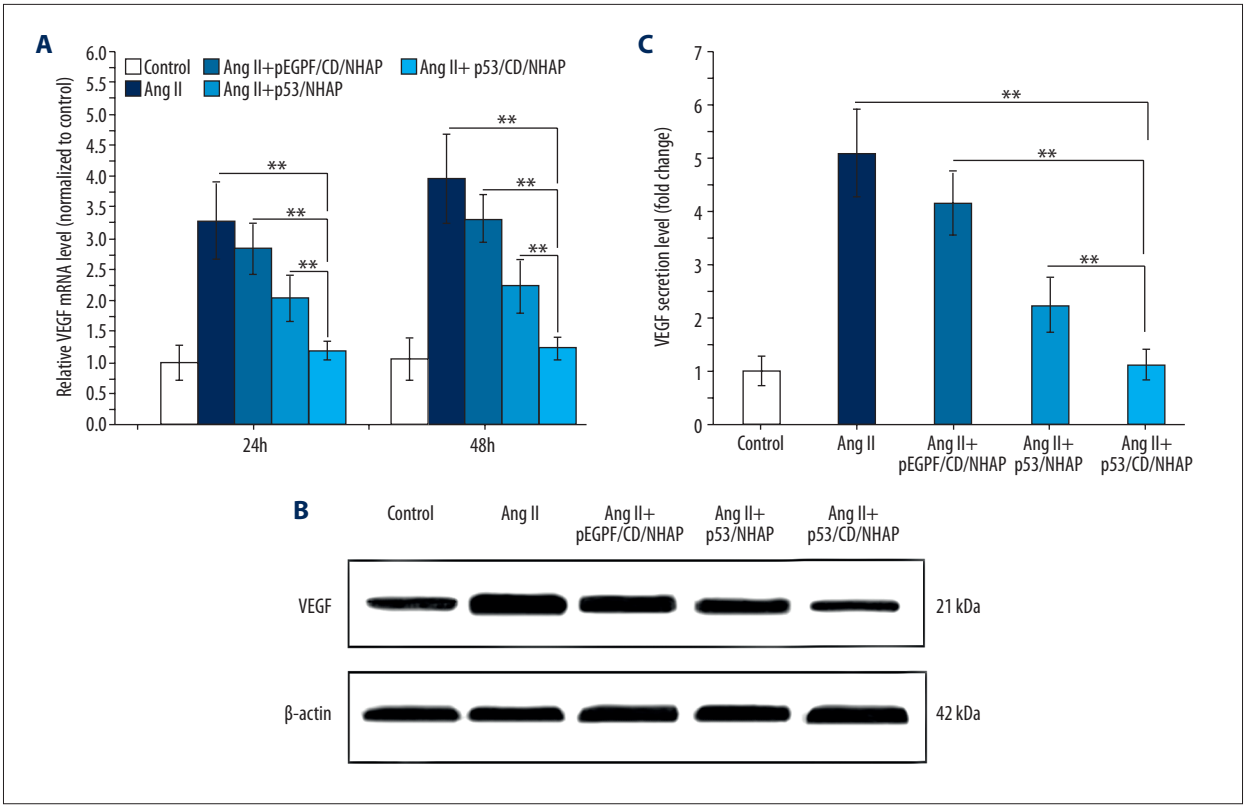

Figure 5. Efficacy of p53/CD/NHAP nanoparticles in suppressing VEGF expression in MCF-7 cells. Ang II (100 nM) was utilized to simulate *in vivo* tumor microenvironment with high Ang II concentration. The untreated cells were taken as a blank control. The suppression of VEGF (**A**) mRNA levels in MCF-7 cells at 24 and 48 h post-treatment were quantified by qRT-PCR. (**B**) The suppression on VEGF protein expression in MCF-7 cells at 48 h after transfection as evaluated by Western blotting assay. (**C**) The secretion of VEGF protein in culture media tested by ELISA kit at 48 h after transfection. Results are expressed as mean ±S.D. (n=5). * P<0.05 and ** P<0.01.

of VEGF. As shown in Figure 5, Ang II remarkably upregulated VEGF expression compared to control (untreated cells), which was set as control to seek the combination anti-angiogenesis efficiency of p53 and CD in p53/CD/NHAP nanoparticles.

As shown in Figure 5A, treatment with p53/NHAPs or pEGFP/CD/NHAPs resulted in the decreased VEGF mRNA level in MCF-7 cells. Above all, it was noted that p53/CD/NHAP nanoparticles further potentiated such a suppression effect in VEGF mRNA level. The VEGF mRNA level in p53/CD/NHAP nanoparticles-treated cells was 3.03-fold lower than that in controls (Ang II-stimulated cells), even compared to the basic level of untreated cells with longer treatment of 48 h. The synergy of these 2 therapeutic components (p53 and CD) was further confirmed by the reduction in VEGF protein using Western blotting assay (Figure 5B). The obtained ELISA analysis results of VEGF expression are consistent with the above-mentioned qRT-PCR and Western blotting assays. As shown in Figure 5C, at 48 h post-transfection, p53/CD/NHAP nanoparticles as a co-delivery system can more significantly downregulated the VEGF secretion from cells induced by Ang II compared with mono-delivery (p53/NHAP and pEGFP/CD/NHAP nanoparticles). These results strongly confirmed that co-delivery of p53 and CD into MCF-7 cells was effectively realized using NHAP nanoparticles. By employing the synergistic effect of p53 and CD, we successfully suppressed the overexpression of angiogenesis-related gene VEGF via different pathways, which might ultimately restrain tumor-associated angiogenesis and lead to preferable anticancer effect.

In vivo anticancer assay

The potential synergistic anticancer efficacy of the p53/CD/NHAP nanoparticles co-delivery system was assessed in MCF-7 xenografted nude mice. As shown in Figure 6A, although tumor growth was suppressed to some extent after administration of mono-delivery system, the combined therapy of p53 and CD appeared to be much more potent when the animals were treated with p53/CD/NHAP nanoparticles. The final tumor volumes in the p53/CD/NHAP nanoparticles group were measured to be 406 ± 56 mm^3. The observations suggested that synergistic anticancer effect of p53 and CD was

Indexed in: [Current Contents/Clinical Medicine] [SCI Expanded] [ISI Alerting System] [ISI Journals Master List] [Index Medicus/MEDLINE] [EMBASE/Excerpta Medica] [Chemical Abstracts/CAS] [Index Copernicus]

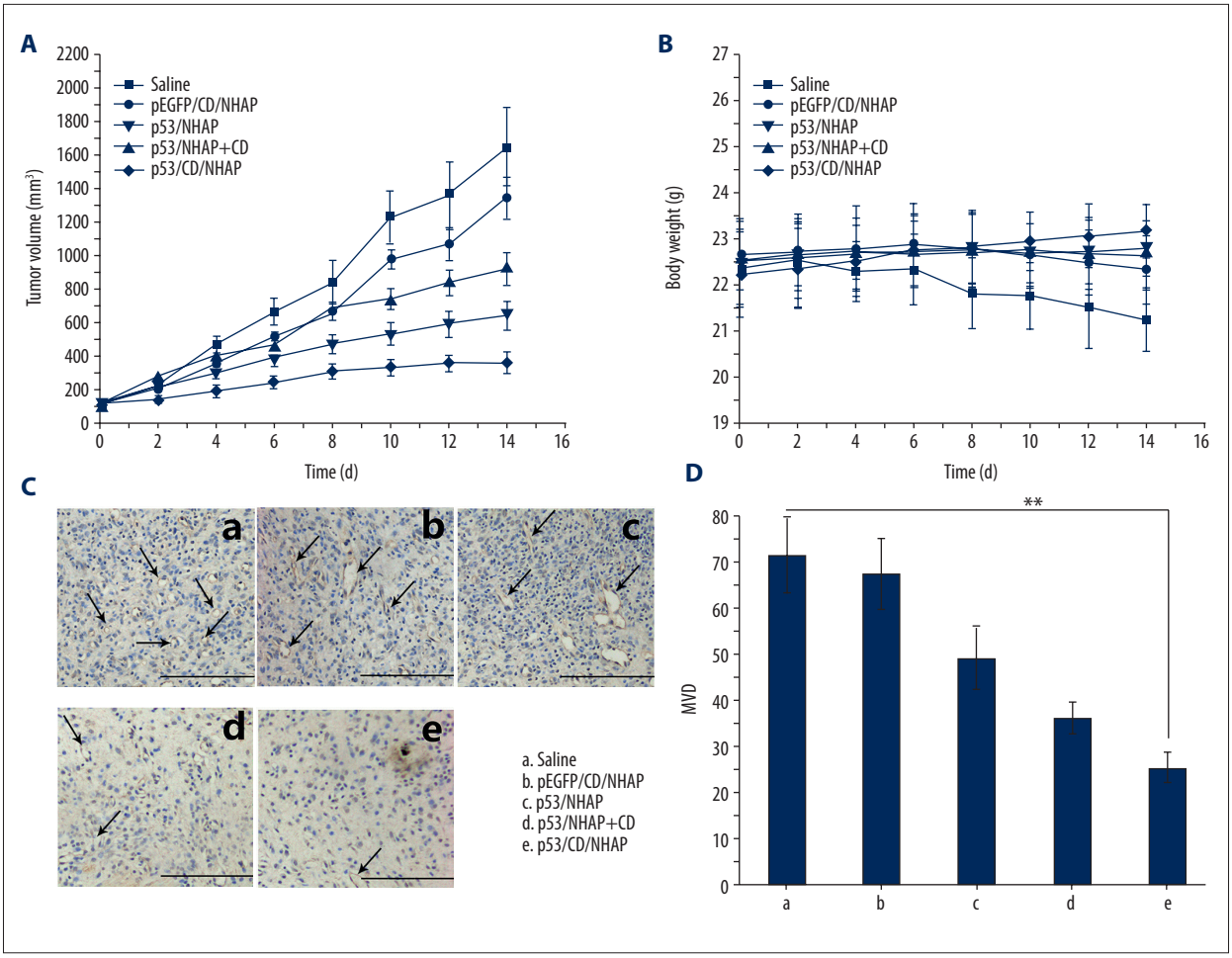

Figure 6. The tumor volume (**A**), body weight (**B**) curve, H&E staining (200×), (**C**) and MVD analysis, and (**D**) of tumor tissues of MCF-7 tumor-bearing BALB/c mice after intravenous administration of saline and different complexes, respectively. The measurement of tumor volume, body weight, and the injection of formulations were repeated every 2 days for 2 weeks. Results are represented as mean ±S.D. (n=6). ** P<0.01. Scale bar: 200 μm.

achieved in the p53/CD/NHAP nanoparticles group. The corresponding body weight variation was also recorded (Figure 6B). It revealed that the untreated mice suffered from a steady decrease in body weight, possibly due to the burden of increasing tumor volume. However, no significant body weight lost was observed in other treatment groups. In the p53/CD/NHAP nanoparticles group, the body weight of mice even increased, suggesting the improved health of treated mice. Moreover, the H&E staining of tumor tissues of mice from each group are displayed in Figure 6C. We observed that tumor tissue from the saline group displayed evident characteristics of cancer cells, with large nuclei and closely packed cells. However, both mono-delivery and co-delivery systems exerted certain anticancer effects, with cancer cell remission being observed. We noted that the p53/CD/NHAP nanoparticles group demonstrated the most powerful anticancer effect with the largest area of cancer cell remission. Further studies on MVD, as a marker of tumor-associated angiogenesis, revealed the tumor angiogenesis suppression as the underlying reason for the synergistic therapeutic effect *in vivo* of CD and p53 gene delivered by a multifunctional co-delivery system. As shown in Figure 6D, MVD in tumors from different groups followed an order: saline > pEGFP/CD/NHAP nanoparticles > p53/NHAP nanoparticles > p53/CD/NHAP nanoparticles, which was consistent with the *in vitro* assays conducted in Section 2. 5. All the above results indicated that breast cancer therapy using p53/CD/NHAP nanoparticles might be a preferable strategy due to the significant angiogenesis inhibition induced by the combination angiogenesis effect of CD and p53. In our future work, we wish to modify p53/CD/NHAP nanoparticles with tumor-targeting ligands (e.g., Folate and antibody) to further enhance their anticancer efficacy.

Indexed in: [Current Contents/Clinical Medicine] [SCI Expanded] [ISI Alerting System] [ISI Journals Master List] [Index Medicus/MEDLINE] [EMBASE/Excerpta Medica] [Chemical Abstracts/CAS] [Index Copernicus]

Conclusions

In this study, well-formed NHAP nanoparticles based on combined angiogenesis therapy for breast cancer were successfully constructed for simultaneously delivery of p53 and CD. The obtained NHAP nanoparticles with suitable amine groups supported effective condensation, and the well-formed p53/CD/NHAP nanoparticles exhibited small particle size, reasonable positive charges, and excellent loading of drug and gene *in vitro*. Moreover, NHAP nanoparticles had almost no cytotoxicity. p53/CD/NHAP nanoparticles potentiated the gene transfection on MCF-7 cells compared to naked plasmid. More importantly, p53/CD/NHAP nanoparticles as a co-delivery system simultaneously delivering p53 and CD and into the same cells achieved stronger inhibitory effect on angiogenesis *in vitro*, possibly resulting from significant downregulation of VEGF expression via different pathways. In particular, our *in vivo* investigation in nude mice bearing MCF-7 xenografts confirmed that our p53/CD/NHAP nanoparticles co-delivery system exerted superior anti-tumor efficacy by a synergistic anti-angiogenic mechanism.

References:

1. Carmeliet P, Jain RK: Angiogenesis in cancer and other diseases. Nature, 2000; 407: 249–57
2. Ferrara N, Kerbel RS: Angiogenesis as a therapeutic target. Nature, 2005; 438: 967–74
3. Fukumura D, Jain RK: Tumor microvasculature and microenvironment: Targets for anti-angiogenesis and normalization. Microvasc Res, 2007; 74: 72–84
4. Hao S, Yan Y, Ren X et al: Candesartan-graft-polyethyleneimine cationic micelles for effective co-delivery of drug and gene in anti-angiogenic lung cancer therapy. Biotechnol Bioproc E, 2015; 20: 550–60
5. Li M, Li Y, Huang X, Lu X: Captopril-polyethyleneimine conjugate modified gold nanoparticles for co-delivery of drug and gene in anti-angiogenesis breast cancer therapy. J Biomater Sci Polym Ed, 2015; 26(13): 813–27
6. Ouyang Q, Duan Z, Jiao G Lei J: A biomimic reconstituted high-density-lipoprotein-based drug and p53 gene co-delivery system for effective anti-angiogenesis therapy of bladder cancer. Nanoscale Res Lett, 2015; 10: 965
7. Shojaei F: Anti-angiogenesis therapy in cancer: Current challenges and future perspectives. Cancer Lett, 2012; 320: 130–37
8. Jiang A, Mammoto T, Jiang E et al: Anti-compression and anti-angiogenic therapy for breast cancer. FASEB J, 2015; 29: 284.2
9. Klauber N, Parangi S, Flynn E et al: Inhibition of angiogenesis and breast cancer in mice by the microtubule inhibitors 2-methoxyestradiol and taxol. Cancer Res, 1997; 57: 81–86
10. Kong W, He L, Richards E et al: Upregulation of miRNA-155 promotes tumour angiogenesis by targeting VHL and is associated with poor prognosis and triple-negative breast cancer. Oncogene, 2014; 33: 679–89
11. Holash J, Wiegand S, Yancopoulos G: New model of tumor angiogenesis: Dynamic balance between vessel regression and growth mediated by angiopoietins and VEGF. Oncogene, 1999; 18(38): 5356–62
12. Vu TH, Shipley JM, Bergers G et al: MMP-9/gelatinase B is a key regulator of growth plate angiogenesis and apoptosis of hypertrophic chondrocytes. Cell, 1998; 93: 411–22
13. Ferrara N, Gerber H-P, LeCouter J: The biology of VEGF and its receptors. Nat Med, 2003; 9: 669–76
14. Wang N, Wang Z-Y, Mo S-L et al: Ellagic acid, a phenolic compound, exerts anti-angiogenesis effects via VEGFR-2 signaling pathway in breast cancer. Breast Cancer Res Treat, 2012; 134(3): 943–55
15. Xiong J, Yang Q, Li J, Zhou S: Effects of MDM2 inhibitors on vascular endothelial growth factor-mediated tumor angiogenesis in human breast cancer. Angiogenesis, 2014; 17: 37–50
16. Zibara K, Awada Z, Dib L et al: Anti-angiogenesis therapy and gap junction inhibition reduce MDA-MB-231 breast cancer cell invasion and metastasis *in vitro* and *in vivo*. Sci Rep, 2015; 5: 12598
17. Chen X, Meng Q, Zhao Y et al: Angiotensin II type 1 receptor antagonists inhibit cell proliferation and angiogenesis in breast cancer. Cancer Lett, 2013; 328(2): 318–24
18. Egami K, Murohara T, Shimada T et al: Role of host angiotensin II type 1 receptor in tumor angiogenesis and growth. J Clin Invest, 2003; 112: 67–75
19. Liang Y, Wu J, Stancel GM, Hyder SM: p53-dependent inhibition of progestin-induced VEGF expression in human breast cancer cells. J Steroid Biochem Mol Biol, 2005; 93(2–5): 173–82
20. Teodoro JG, Parker AE, Zhu X, Green MR: p53-mediated inhibition of angiogenesis through up-regulation of a collagen prolyl hydroxylase. Science, 2006; 313: 968–71
21. Ventura A, Kirsch DG, McLaughlin ME et al: Restoration of p53 function leads to tumour regression *in vivo*. Nature, 2007; 445: 661–65
22. Xu Q, Xia Y, Wang C-H, Pack DW: Monodisperse double-walled microspheres loaded with chitosan-p53 nanoparticles and doxorubicin for combined gene therapy and chemotherapy. J Control Release, 2012; 163(2): 130–35
23. Goldstein I, Marcel V, Olivier M et al: Understanding wild-type and mutant p53 activities in human cancer: New landmarks on the way to targeted therapies. Cancer Gene Ther, 2011; 18: 2–11
24. Yamakuchi M, Lotterman CD, Bao C et al: P53-induced microRNA-107 inhibits HIF-1 and tumor angiogenesis. Proc Natl Acad Sci USA, 2010; 107: 6334–39
25. Zhang L, Yu D, Hu M et al: Wild-type p53 suppresses angiogenesis in human leiomyosarcoma and synovial sarcoma by transcriptional suppression of vascular endothelial growth factor expression. Cancer Res, 2000; 60: 3655–61
26. Hare JI, Moase EH, Allen TM: Targeting combinations of liposomal drugs to both tumor vasculature cells and tumor cells for the treatment of HER2-positive breast cancer. J Drug Target, 2013; 21: 87–96
27. Bao X, Wang W, Wang C et al: A chitosan-graft-PEI-candesartan conjugate for targeted co-delivery of drug and gene in anti-angiogenesis cancer therapy. Biomaterials, 2014; 35: 8450–66
28. Wang C, Li M, Yang T et al: A self-assembled system for tumor-targeted co-delivery of drug and gene. Mater Sci Eng C Mater Biol Appl, 2015; 56: 280–85
29. Zheng C, Zheng M, Gong P et al: Polypeptide cationic micelles mediated co-delivery of docetaxel and siRNA for synergistic tumor therapy. Biomaterials, 2013; 34: 3431–38
30. Chen AM, Zhang M, Wei D et al: Co-delivery of doxorubicin and Bcl-2 siRNA by mesoporous silica nanoparticles enhances the efficacy of chemotherapy in multidrug-resistant cancer cells. Small, 2009; 5: 2673–77
31. Xiong H, Du S, Ni J et al: Mitochondria and nuclei dual-targeted heterogeneous hydroxyapatite nanoparticles for enhancing therapeutic efficacy of doxorubicin. Biomaterials, 2016; 94: 70–83
32. Zhu S, Huang B, Zhou K et al: Hydroxyapatite nanoparticles as a novel gene carrier. J Nanopart Res, 2004; 6: 307–11
33. Matsoukas M-T, Cordomí A, Ríos S et al: Ligand binding determinants for Angiotensin II type 1 Receptor from Computer Simulations. J Chem Inf Model, 2013; 53(11): 2874–83
34. Xu H, Jiang Y, Wei D, Gai X: Amine functionalized hydroxyapatite nanoparticles for anti-angiogenesis gene therapy of breast cancer. IET Micro & Nano Letters, 2016; 11(8): 416–19
35. Wang C, Bao X, Ding X et al: A multifunctional self-dissociative polyethyleneimine derivative coating polymer for enhancing the gene transfection efficiency of DNA/polyethyleneimine polyplexes *in vitro* and *in vivo*. Polymer Chemistry, 2015; 6: 780–96
36. Wang C, Chen S, Yu Q et al: Taking advantage of the disadvantage: Employing the high aqueous instability of amorphous calcium carbonate to realize burst drug release within cancer cells. Journal of Materials Chemistry B, 2017; 5: 2068–73

Indexed in: [Current Contents/Clinical Medicine] [SCI Expanded] [ISI Alerting System] [ISI Journals Master List] [Index Medicus/MEDLINE] [EMBASE/Excerpta Medica] [Chemical Abstracts/CAS] [Index Copernicus]

37. Chen Q-R, Kumar D, Stass SA, Mixson AJ: Liposomes complexed to plasmids encoding angiostatin and endostatin inhibit breast cancer in nude mice. Cancer Res, 1999; 59: 3308–12

38. Cuong NV, Jiang JL, Li YL et al: Doxorubicin-loaded PEG-PCL-PEG micelle using xenograft model of nude mice: Effect of multiple administration of micelle on the suppression of human breast cancer. Cancers (Basel), 2010; 3(1): 61–78

39. Lee M, Nah J-W, Kwon Y et al: Water-soluble and low molecular weight chitosan-based plasmid DNA delivery. Pharm Res, 2001; 18: 427–31

Indexed in: [Current Contents/Clinical Medicine] [SCI Expanded] [ISI Alerting System] [ISI Journals Master List] [Index Medicus/MEDLINE] [EMBASE/Excerpta Medica] [Chemical Abstracts/CAS] [Index Copernicus]